STATUS OF THE VARIABLE DIAMETER CENTERBODY INLET PROGRAM

J. D. Saunders and A.A. Linne
NASA Lewis Research Center
Cleveland, Ohio

First Annual
High Speed Research Workshop
May 14-16, 1991

THE VARIABLE DIAMETER CENTERBODY INLET

The Variable Diameter Centerbody, (VDC), inlet is an ongoing research program at the Lewis Research Center. The VDC inlet is a mixed compression, axisymmetric inlet that has potential application on the next generation supersonic transport. This inlet was identified as one of the most promising axisymmetric concepts for supersonic cruise aircraft during the SCAR program in the late 1970's, reference 1. Some of its features include high recovery, low bleed, good angle-of-attack tolerance and excellent engine airflow matching, figure 1. These features have been demonstrated at Lewis in the past by the design and testing of fixed hardware models, references 2 to 5. A current test program in the LeRC 10'x10' Supersonic Wind Tunnel, (SWT), will attempt to duplicate these features on model hardware that actually incorporates a flight-like variable diameter centerbody mechanism.

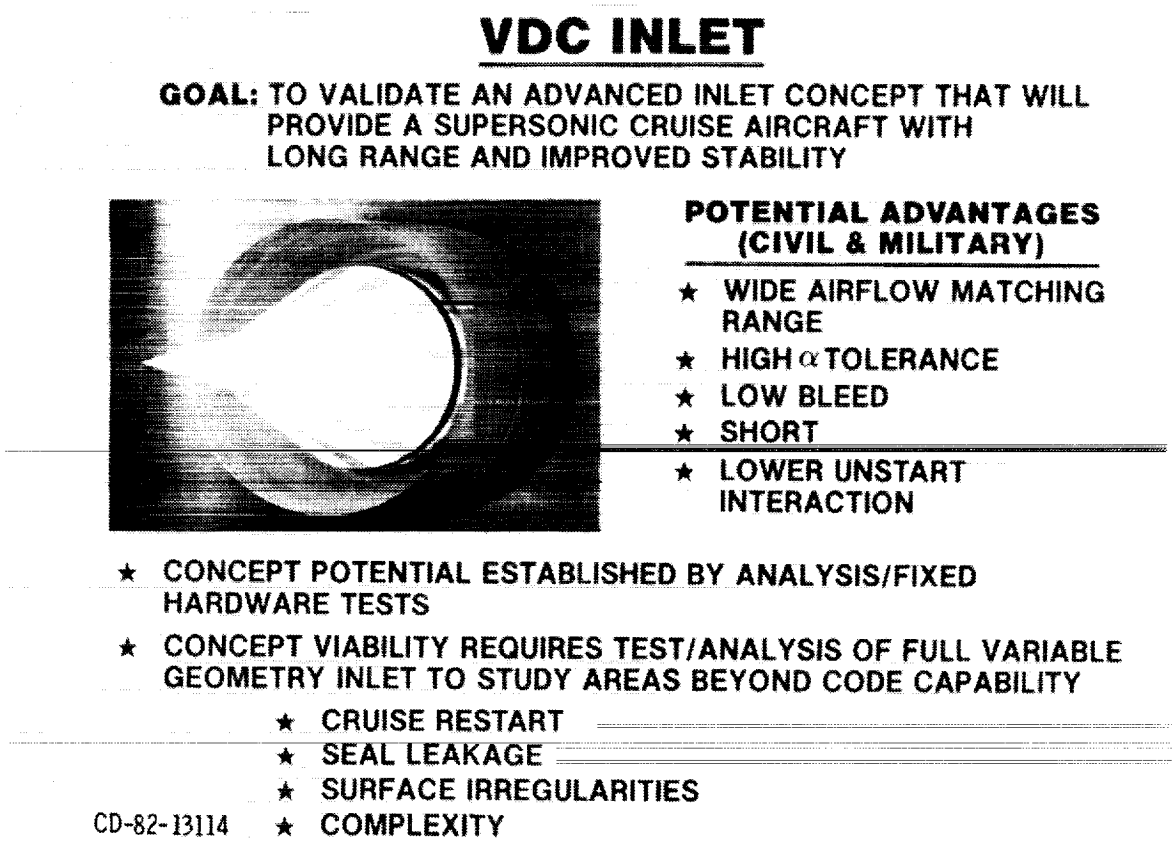

FIGURE 1. VDC Inlet

VDC OVERVIEW

This paper is developed around two major efforts to develop a variable diameter centerbody inlet: an experimental program and an analytical study using state of the art computational fluid dynamics tools, (CFD), figure 2..

The efforts to demonstrate the VDC concept experimentally date back nearly 25 years. This history as well as the original design philosophy behind the inlet will be briefly discussed. Results from the early testing will be referenced and discussed further in the analytical portion of the paper. The upcoming test program will then be outlined.

The analytical effort has centered around the use of computer codes that solve the Full Navier-Stokes, (FNS), equations for a viscous compressible fluid. Lower level Euler analysis was also found useful in screening inlet geometry for off-design performance. Together, these analytical efforts have served to prepare for the future testing.

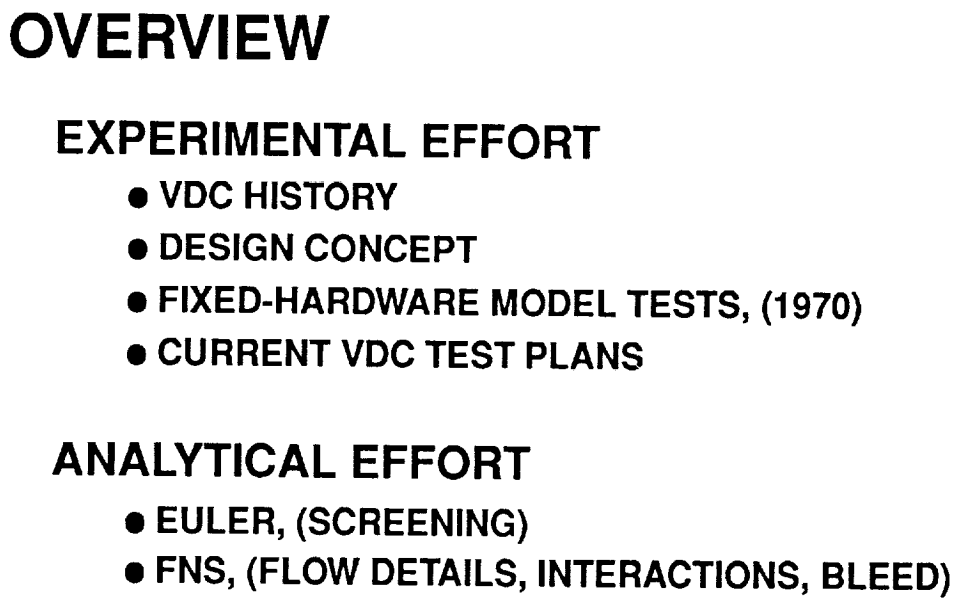

FIGURE 2. VDC Overview

PROGRAM HISTORY

An outcome of the supersonic cruise research (SCR) program identified the VDC inlet as an important technology thrust to continue funding, reference 6. It is an axisymmetric inlet of a mixed compression design that provides high performance at its cruise Mach number of 2.5. Aerodynamic testing of the concept was done with fixed hardware in the early 1970's and verified the high expected performance of this concept.- This model was tested in the LeRC 10'x10' Supersonic Wind Tunnel at Mach numbers of 2.5 and 2.0. For economic reasons the mechanical design of that test inlet was simplified to incorporate fixed centerbody configurations. A photo of the model installed in the 10'x10' SWT is shown in figure 3.

Mechanical design of the VDC inlet with the variable geometry began in 1982 and a complete set of drawings was finished in mid-1984. Unfortunately, programmatic restructuring canceled the program with only a fraction of the hardware fabricated or procured. The High Speed Research program has revived interest in a commercial supersonic aircraft in general and this inlet program in particular. The test program in the LeRC 10'x10' SWT is slated to begin in the summer of 1992.

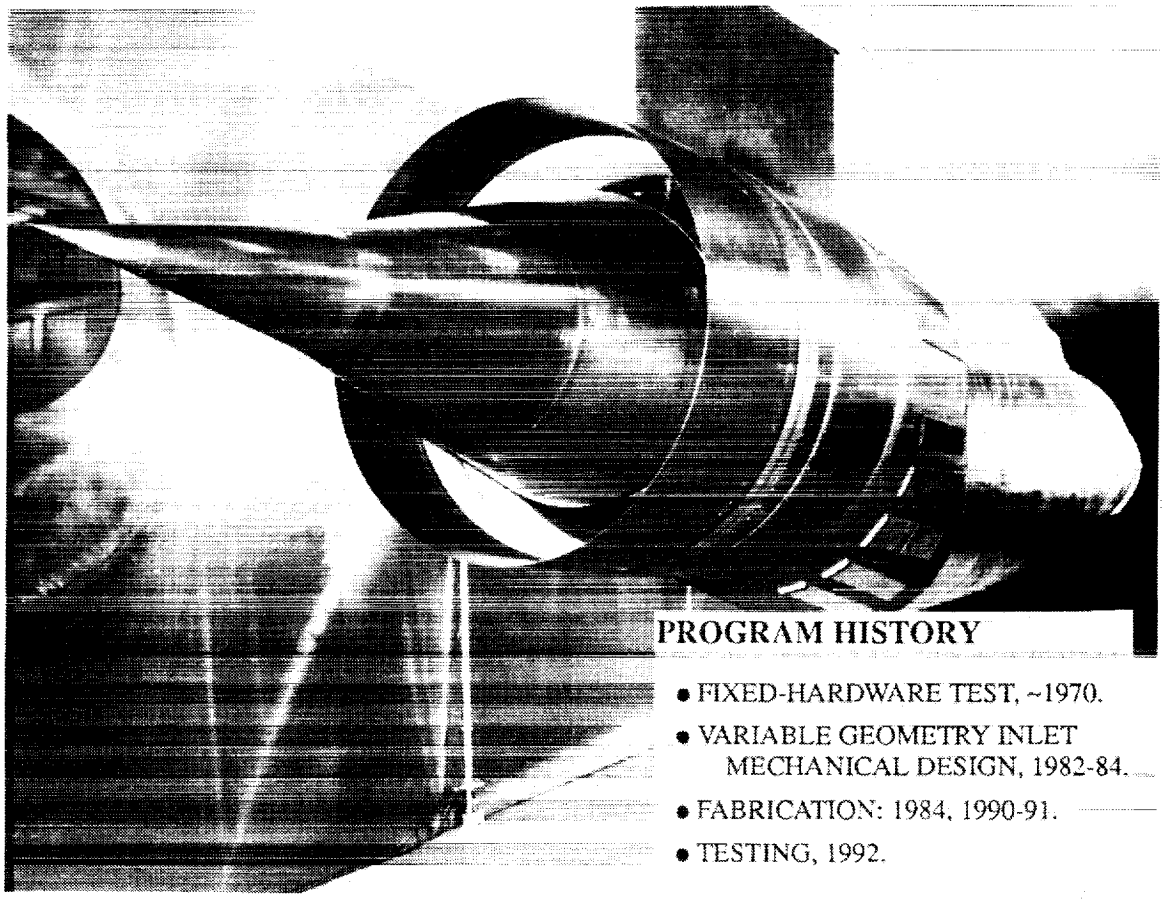

FIGURE 3. Program History

FIXED-HARDWARE TESTING

The fixed-hardware inlet model was sized and tested with a TF-30 turbofan engine. The cowl lip radius, Rc, was 18.68 inches. Other aspects of the inlet design include the variable diameter centerbody and a focussed cowl compression on a slotted bleed region in the centerbody. The variable diameter centerbody allows large variations in throat area and airflow to provide good compatibility with the engine. The focussed cowl compression minimizes bleed flow requirements and reduces the inlet length and resulting weight. An schematic view of this model is also shown in figure 4. The model had centerbody and cowl bleed for performance and shock stability and overboard bypass air for engine matching. Vortex generators were installed downstream of the throat to prevent separation in the subsonic diffuser.The essential features of the inlet design incorporate a bicone centerbody of 12.5° and 18.5° half angle cones and an initial internal cowl angle of 2°. The design philosophy for this mixed compression inlet is to utilize a bicone spike to provide the maximum external compression compatible with high total pressure recovery and low cowl drag. As a result, 45 percent of the supersonic area contraction is internal for the Mach 2.5 design condition.

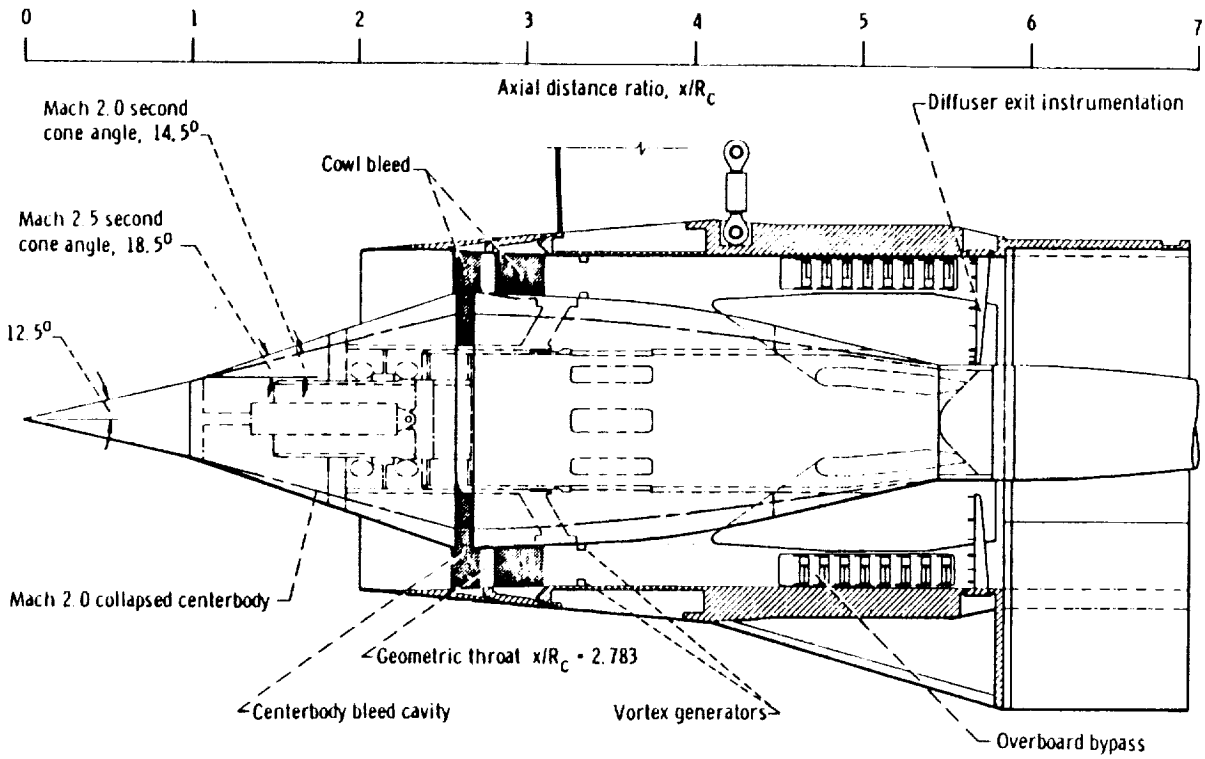

FIGURE 4. Fixed-Hardware Testing

VDC INLET MODEL DESIGN

Essentially, the Variable Diameter Centerbody inlet contours were developed with the same aerodynamic design philosophy as the earlier fixed-geometry model. The supersonic diffuser cowl and centerbody geometries were designed with a Method of Characteristics, (MOC), computer code, reference 7. The characteristic mesh from the supersonic design code is shown in figure 5.

Also shown are the assembly details of the VDC inlet model. The VDC inlet incorporates an umbrella-like mechanism to create a variable diameter centerbody. The mechanism allows the centerbody to change diameter while maintaining good aerodynamic flow surfaces at off-design diameters. Both the variable diameter mechanism as well as centerbody spike translation are hydraulically actuated. Centerbody bleed and bypass airflows are also remotely variable. Relative positioning of the biconic portion to the contoured subsonic diffuser portion of the centerbody is manually adjustable. Bleed on the internal cowl surface near the inlet throat is also available. The variable-hardware model is sized for a relatively small J-85 turbojet engine and, therefore, is less than half the size of the fixed-hardware model, Rc = 8.31". The supersonic diffuser of the J-85 sized VDC inlet is geometrically scaled from the fixed hardware model. The subsonic diffusers are slightly different but retain nearly the same length to diameter and area ratios.

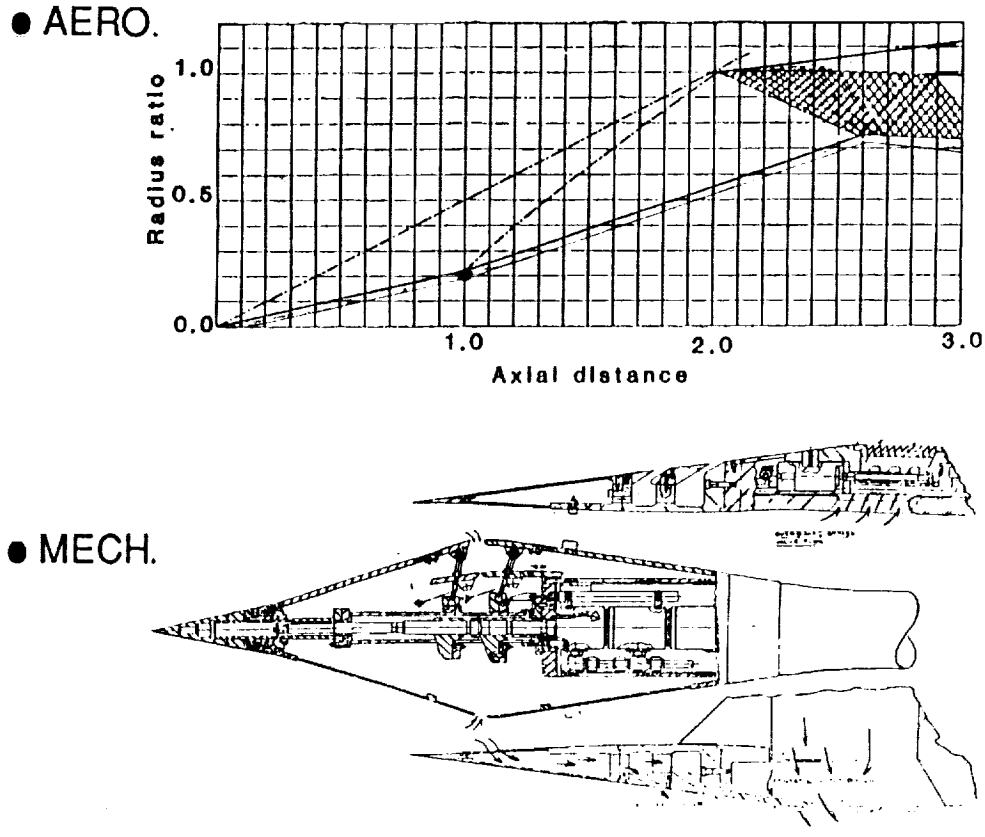

FIGURE 5. VDC Inlet Model Design

VDC INLET FORWARD 'LEAVES'

A photo of the assembled mechanism for the second cone of the supersonic diffuser is shown below. The mechanism is made of a series of separate 'leaves' that are jointed at the minimum diameter where they attach to the 12.5^{o} cone. The edges of the leaves are slotted to provide seals along the leaves. This seal prevents the relatively high pressure centerbody bleed air contained within the leaves from disturbing the supersonic airflow flowing along the outer leaf surfaces. Preliminary leakage tests of these seals suggests the maximum leakage rate will by a fraction of 1% of the supersonic capture flow.

The aft set of 'leaves', which constitute the contoured subsonic diffuser portion of the centerbody, as well as many other parts are currently being fabricated. This inlet concept strives for superior inlet performance at the drawback of increased mechanical complexity.

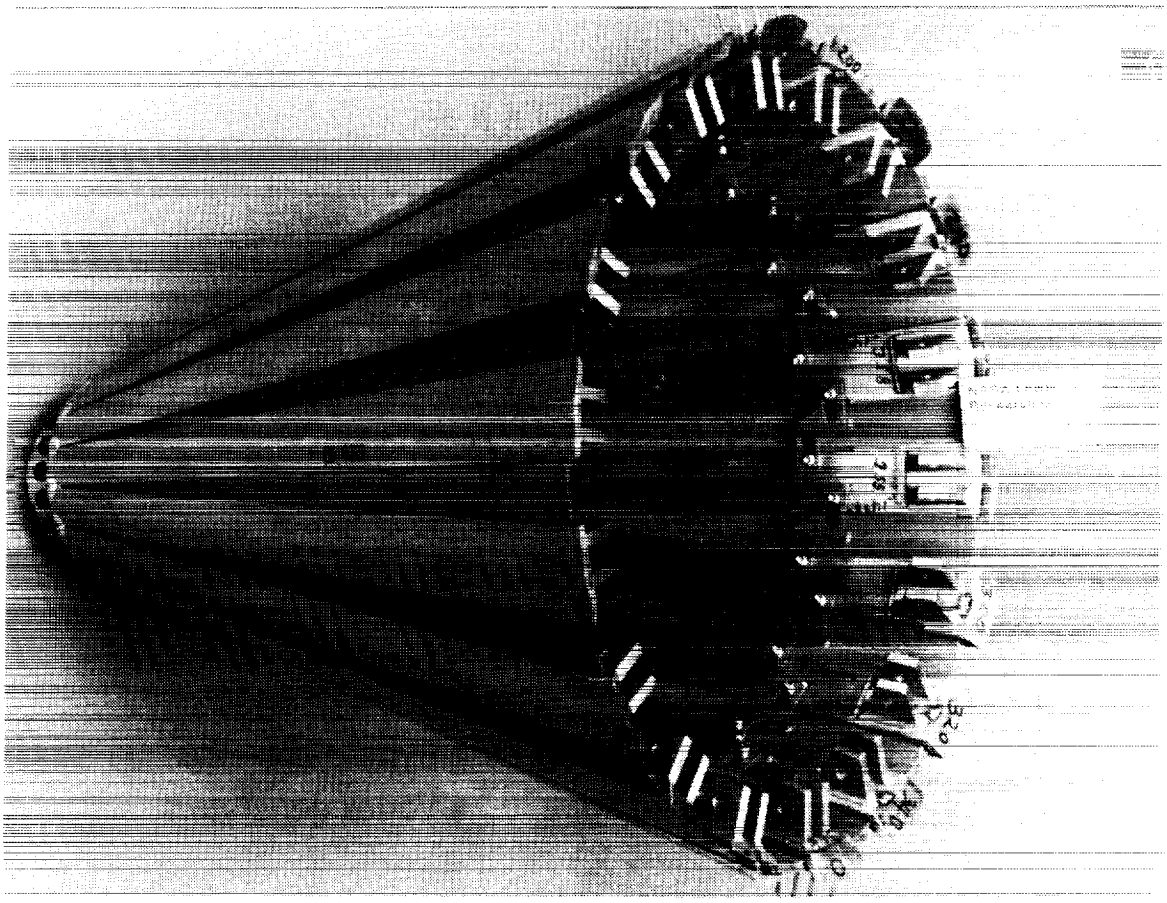

FIGURE 6. Forward leaf Assembly

TEST PROGRAM SCHEDULE & GOALS

The schedule for the test program is shown in figure 7. Hardware, instrumentation and assembly should be complete early next year, (1992). Approximately two months of testing are initially planned. The major test goals are also listed. Inlet performance will obtained and compared to the earlier fixed-hardware model tests. In this initial testing the inlet will be mounted ahead of a mass flow plug metering device that both measures mass flow through the inlet and provides backpressure, thus simulating the effect of an engine. Other important testing parameters include the variable diameter, (second cone angle), centerbody bleed rate, centerbody translation and angle of attack. Secondary parameters include cowl bleed rate and configuration, centerbody bleed slot geometry, bypass flow rate, and the effect of vortex generators in the subsonic diffuser. A final goal is to demonstrate the viability of the variable geometry concept under flight loads with flight-like mechanisms.

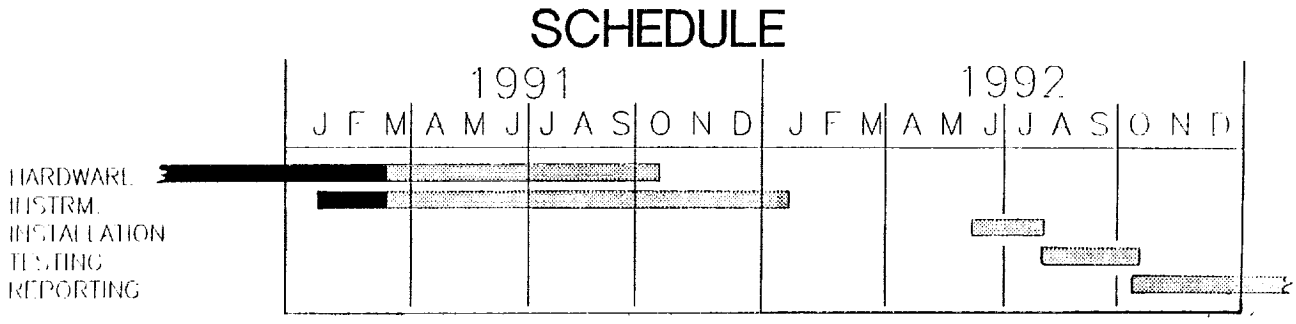

TEST GOALS

- AERODYNAMIC PERFORMANCE
  - Recovery vs. Capture
  - Off-design performance
  - Bleed configurations and flows
  - Angle of Attack
  - Bypass flow rate
  - Vortex generators
- MECHANICAL OPERABILITY

FIGURE 7. Test Schedule and Goals

CFD ANALYSIS

This analytical study was undertaken, in part, to prepare for the experimental test program. Input for the analysis was setup for the fixed-hardware, TF-30 sized, inlet. Comparison between experimental test results from the fixed geometry model and various computational fluid dynamic analyses will be made, figure 8.

Preliminary analysis using subsets of the full Navier-Stokes equations was done to determine off-design performance and prepare for the use of the FNS codes. As mentioned, the original supersonic inlet lines were developed using a MOC design program. Subsequent analysis continued to use MOC codes to determine off-design performance, (performance at flight Mach numbers below design). Additionally, a quick study was done with a Parabolized Navier-Stokes code to determine the effect of turbulent viscosity but was unsuccessful due to problems with computational grid development for this code. Results from these early efforts as well as other CFD studies, references 12 to 21, helped to guide further work with the FNS codes.

Two FNS computer codes, called PROTEUS and PARC, references 9 and 10, were used to solve the two-dimensional, axisymmetric, Reynolds-averaged, steady compressible Navier-Stokes equations for the flow through the VDC inlet at its design Mach number of 2.5. Both codes have flexible boundary conditions, good documentation, Baldwin-Lomax turbulence models and options to solve for inviscid or laminar viscous flow solutions. The codes are essentially very similar, but subtle differences in their implementation and user interface proved both codes to be useful. Problems in grid refinement, obtaining started inlet flow, and bleed modeling had to be overcome prior to simulating critical inlet operation.

The initial flow field was set to Mach 2.5 freestream conditions throughout the flow field and zero velocities at the inlet's centerbody and cowl. The compressor face boundary is initially set as an extrapolation condition. This setup should allow the inlet shocks to develop, the flow to compress nearly to critical conditions in the throat and then reaccelerate to supersonic conditions down through the diffuser and out the compressor face boundary. Once this flow solution reaches steady state conditions, various levels of outflow "back" pressure are applied to position the normal shock downstream of the throat. An extreme sensitivity of the flow simulation to exit backpressure was discovered with time marching FNS codes.

This back-pressuring process is not straight forward. Since the change in back-pressure, (or any boundary condition change), occurs across some element of computational time, the change is an inherently unsteady event. Essentially, a change in pressure corresponds to an increase in momentum due to the suddenness or acceleration of pressure change. If the pressure change occurs over a single iteration step as it does with the PARC code, a large transient shock forms whose strength is inversely proportional to the computational time-step. This shock is analogous to an inlet hammershock that occurs in real supersonic inlet-engine systems when the engine stalls, references 11 to 13.

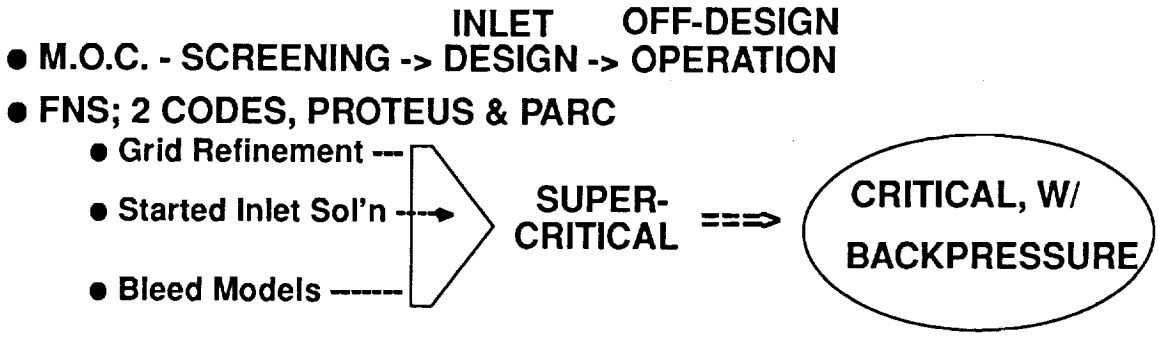

FIGURE 8. CFD Analysis

MOC OFF-DESIGN PERFORMANCE

Prior to analysis with full Navier-Stokes codes, lower level analysis was conducted using a Method-of-Characteristics, (MOC), code. As mentioned, the original supersonic inlet design was done with the aid of a MOC code. Further analysis was conducted using another MOC code, reference 8, to determine performance of the inlet at freestream Mach numbers below the cruise Mach number of 2.5.

This off-design analysis is presented in figure 9. It shows the necessary angle of the second cone to maintain started inlet flow according to two constraints. The first constraint maintains the shock from the cowl lip on the shoulder or bleed slot of the centerbody. The second constraint maintains a certain Mach number in the inlet throat. Several throat Mach numbers are plotted representing different trades between performance and stability. For a throat Mach number of 1.2 the inlet would have the highest performance but least stability and may in fact be difficult to start. A throat Mach number of 1.4 is more stable but less efficient. Areas of the operating map below the constraint curves would have increasingly lower distortion, better efficiency but lower angle of attack and stability. Eventually, the decrease in stability will lead to inlet unstart.

Note that at a second cone angle of 18.5^{o} the shocks on shoulder and throat Mach number of 1.3 constraints converge at the design freestream Mach number of 2.5. The convergence verifies the design methodology. The shock-on-shoulder constraint lies between throat Mach numbers of 1.2 and 1.3 at off-design freestream Mach numbers down to Mach 2.0. Off-design performance for this inlet should be fairly good but increasingly less stable. The constraint curves demonstrate a well-behaved relation between freestream Mach number and second cone angle which is useful information in the eventual testing and analysis of the inlet's off-design performance. Finally, note that at the freestream Mach number of 2.0, the shock-on-shoulder and throat Mach number constraints converge at a second cone angle of 14.5^{o}, which is also the geometry tested in the fixed hardware tests.

This operating map represents over 30 test cases; a task that points out the usefulness of Euler analysis in screening large number of configurations.

FIGURE 9. Off-Design Performance Map

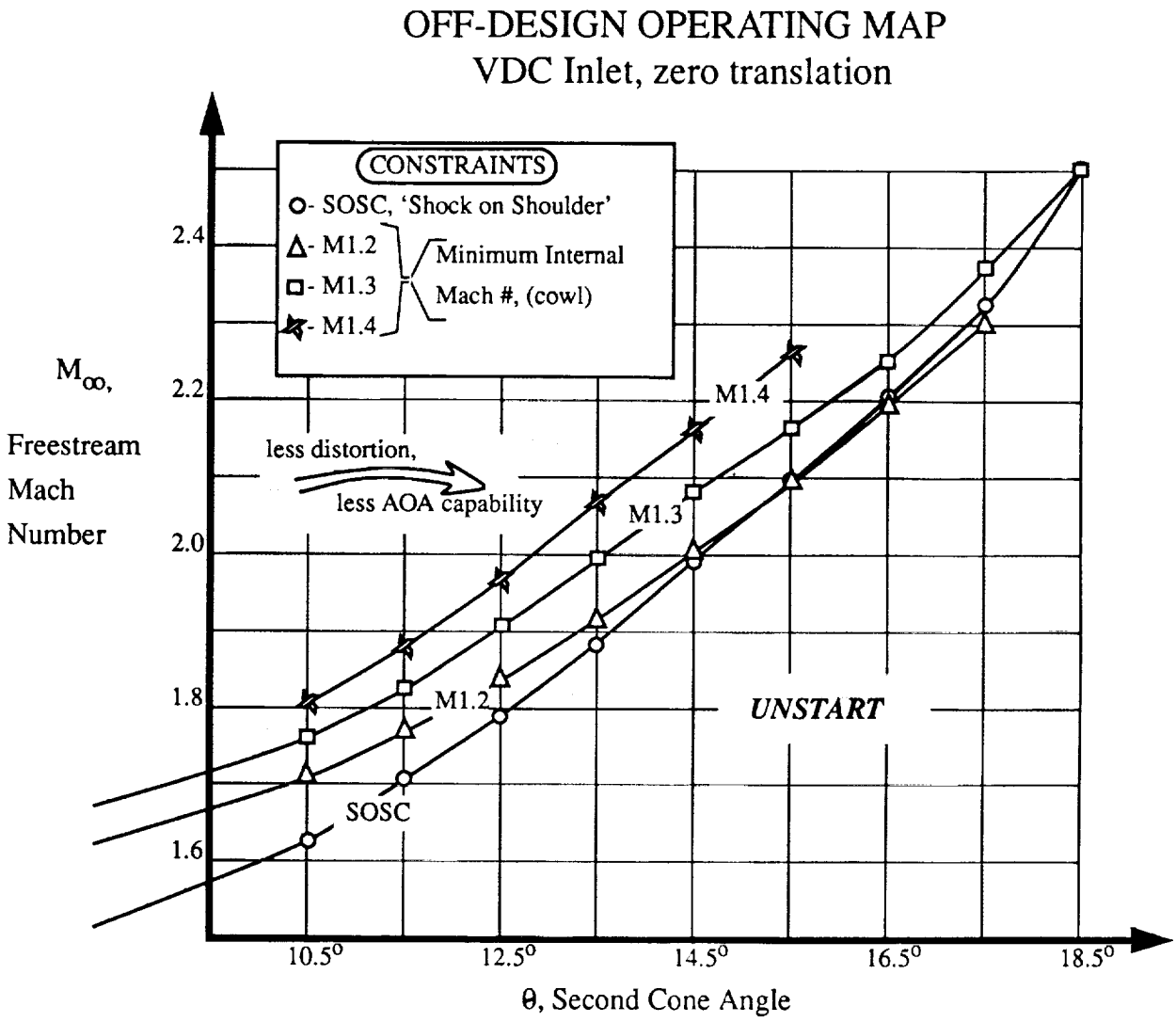

FIGURE 9. Off-Design Performance Map

FNS CODES, EULER RESULTS

Initial results were obtained using the Euler subset of the FNS equations and using a fairly conventional mesh. The mesh for this case was uniformly distributed in the radial direction and slightly packed in the streamwise direction. The grid dimensions were 99x99.

Mach number contours are shown in figure 10. Examination of the contours shows significant shock wave smearing in the physical domain. In fact, the cowl shock is not sharply defined, and the entire cowl compression appears to be distributed both well upstream and downstream of the shoulder. (Recall that the inlet design was for shock cancellation and focussed cowl compression at the centerbody shoulder). Because the cowl shock wave is not crisply resolved, the shock/boundary layer/bleed interaction on the centerbody would be poorly modeled with this grid.

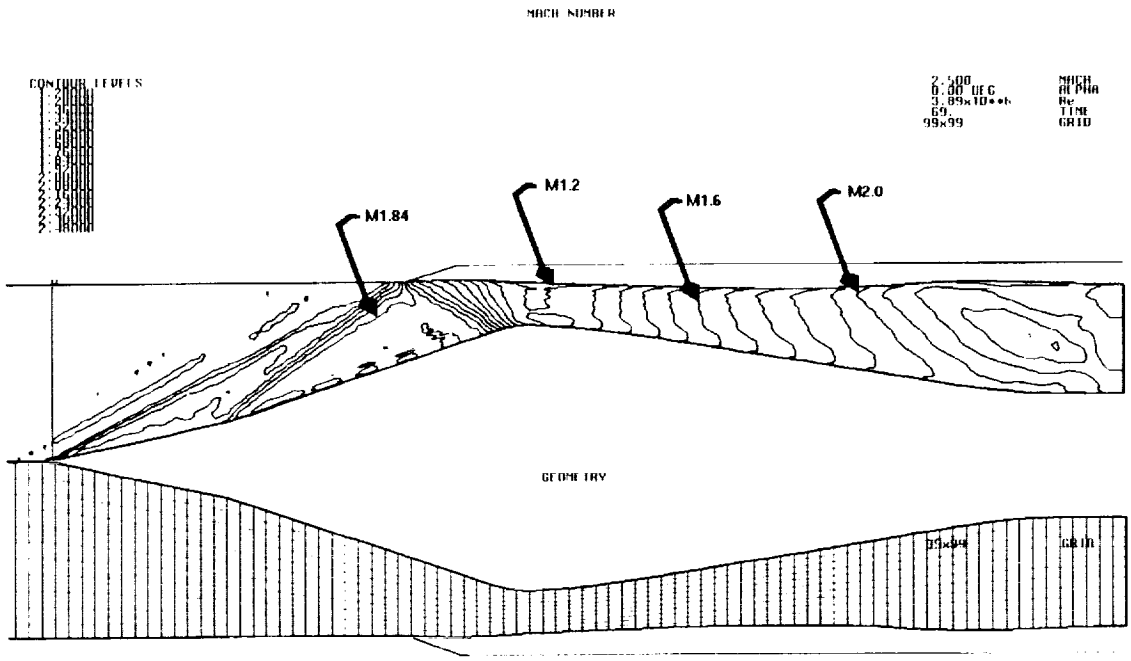

FIGURE 10. Euler Results

REFINED GRID RESULTS

An effort in skewing and packing the grid points as well as adding more grid points to the calculation domain was strongly motivated by the previous result. Figure 11 shows the effect of grid refinement on intermediate FNS-inviscid results. Although both of these calculations eventually unstarted, the sharpness of the shock waves is clearly much better for the skewed, packed mesh.

Without bleed and with the refined mesh, both Euler and laminar solutions predicted the cowl shock to intersect forward of the shoulder, causing boundary layer separation on the centerbody. The separation enlarged with further iterations, and as mentioned, cause the inlet flowfield to unstart. This prediction compares to the experimental results that indicated ~2% bleed flow rate through the centerbody bleed slot was needed to keep the inlet started.

Together the results indicate that even with the refined mesh, the shocks are smeared forward of their inviscid positions, causing adverse interaction that prevents started inlet flow. Analysis without bleed was therefore de-emphasized and bleed modeling was implemented into the analyses' boundary conditions.

While the bleed models were being implemented into the codes, one last attempt was made to develop a started inlet configuration.For this case, the inlet geometry was modified by translating the cowl slightly downstream relative to the centerbody. This change reduced the internal contraction ratio and also moves the cowl shock downstream of the shoulder, both of which aid inlet starting. Initial cases were developed for Mach 3 freestream flow. Started inlet flow was achieved for this case, but was of limited practical interest. The calculated flowfield did provide useful initial conditions for subsequent cases using the design geometry and centerbody bleed

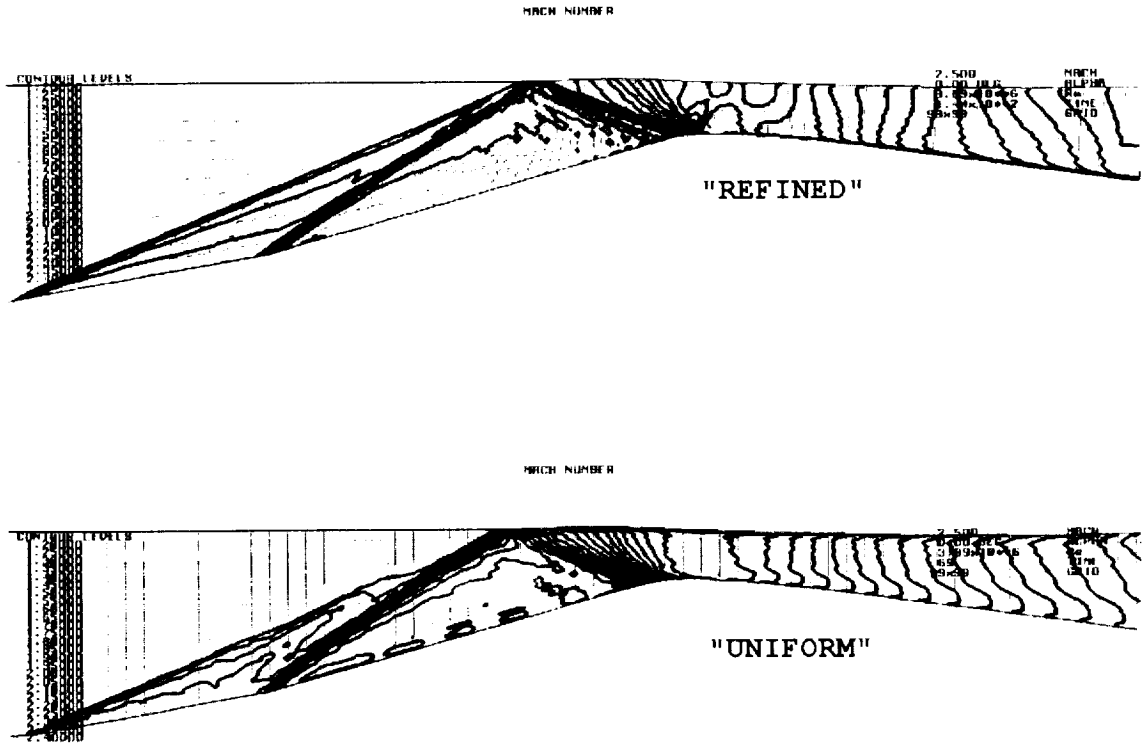

FIGURE 11. Refined Grid Results

DESIGN CASE, SUPERCRITICAL

With the bleed model setup, the next case used the design inlet geometry but at the design Mach number of 2.5. The bleed rate was set at ~6% which is conservatively much greater than the experimentally obtained optimum rate of ~2%. Both FNS codes were run for the same case and the comparison of Mach number contours is shown in figure 12. The contours are for a detailed region through the inlet throat. Upstream of the centerbody bleed slot, agreement between the two codes is good. The cowl shock hits slightly forward of the shoulder causing a small separation. The cowl shock reflects from this separation and then crosses back to the cowl surface. The reflection on the cowl surface is of sufficient strength to separate the cowl boundary layer and cause a Mach reflection. Downstream of the Mach reflection, a small subsonic pocket in the flow is formed. The PARC code resolves this phenomena more crisply than the PROTEUS code. The shock continues to reflect and coincides with the oblique shock at the aft end of the bleed slot on the centerbody surface.

These results are for a low level of back pressure, (supercritical inlet operation), which forces a terminal shock to form near the end of the centerbody bleed slot. In the PROTEUS analysis, this oblique is weak and the flow remain supersonic downstream. The PARC code predicts a strong oblique shock that coalesces with the terminal to generate subsonic flow. For both code predictions, the terminal shock is locally unsteady, (this result will be discussed later).

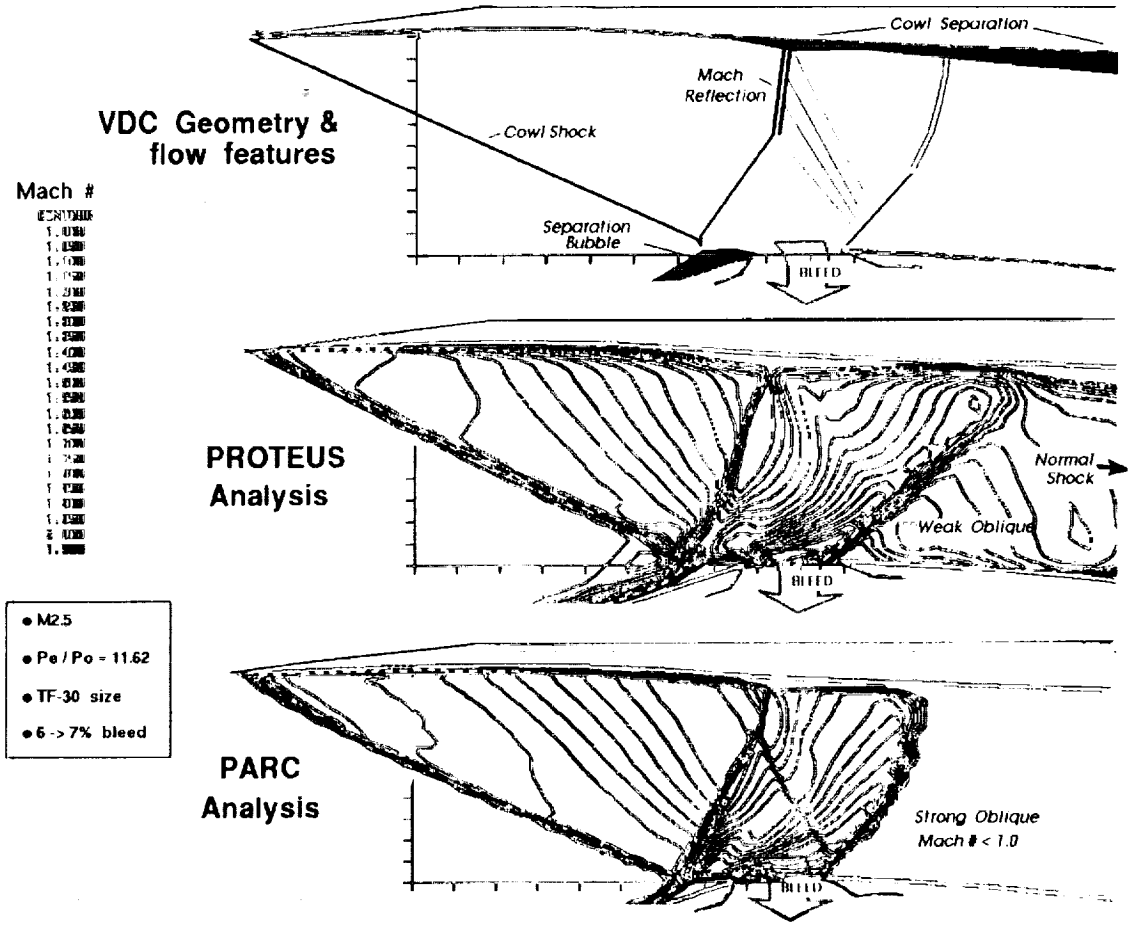

FIGURE 12. Design Case, Supercritical

PARTICLE TRACES, DESIGN CASE

To further display the features of this flow, figure 13 shows the particle traces for this case from the PARC code analysis. The small separation forward of the centerbody shoulder bleed slot and the bleed flow exiting through the slot are clearly evident. This case was done with slightly less bleed flow at 2%, so its solution is directly relatable to the data. The experimental data deviates from the inviscid MOC prediction slightly forward of the shoulder, reference 1. The deviation was attributed to small separation existing in this region, and thus qualitatively verifies the FNS predictions. The result also suggested a need for additional static pressure instrumentation to better quantify the extent of the separation.

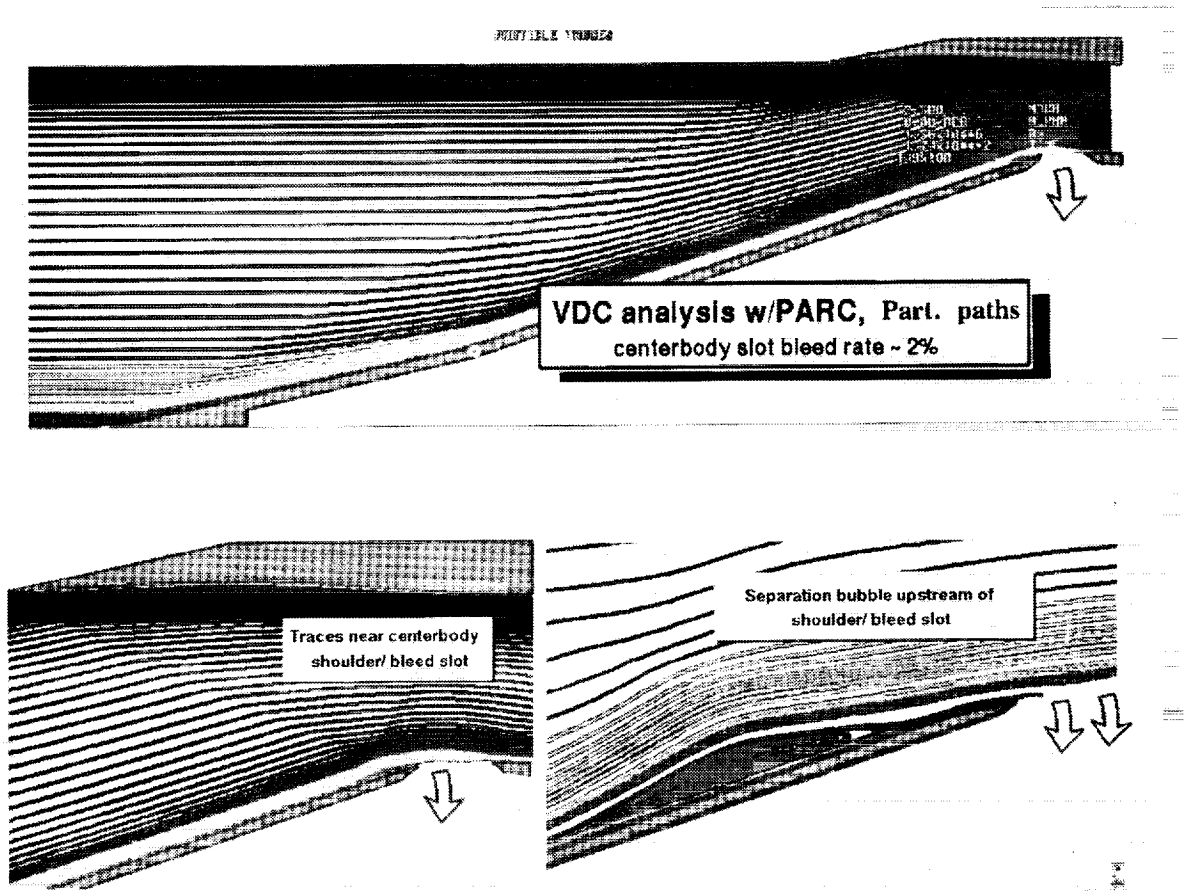

FIGURE 13. Particle Traces

COMPARISON TO DATA

Figure 14 shows the results of the comparison of pitot pressures between the experiment and numerical solution. The locations of various rakes are shown on figure 16. Comparison is excellent for the cowl throat rake. The flow on the cowl to this point is unaffected by separations and by the centerbody bleed, so boundary layer growth and oblique shock pressure level should be correctly modeled by the code. Pitot pressure profiles for the other two rakes show moderate agreement. These rakes are downstream of separations and the bleed slot. Therefore, they are strongly affected by phenomena that are, at best, only approximately simulated by the turbulence model and the bleed boundary condition.

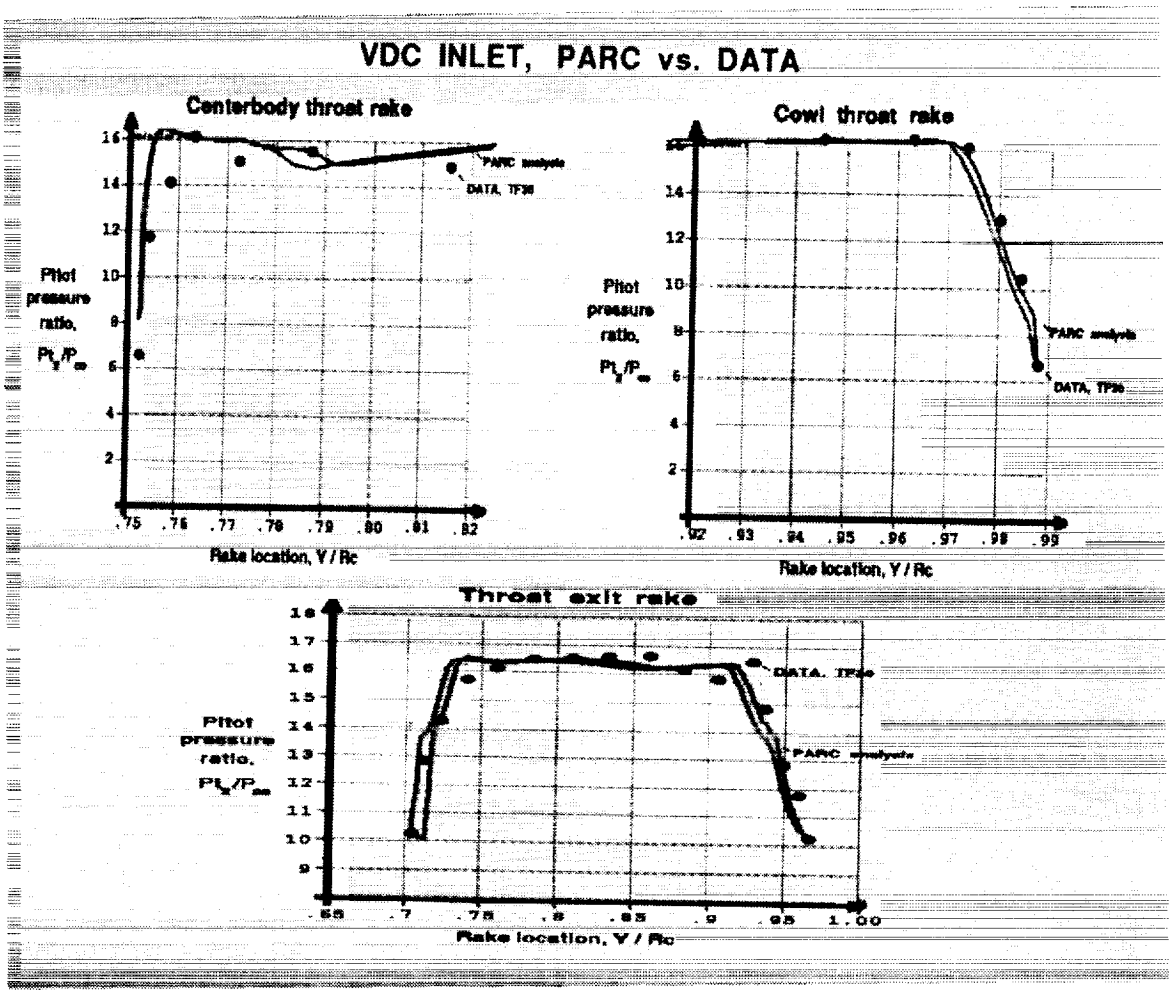

FIGURE 14. Comparison to Data

BACKPRESSURE AND FLOW OSCILLATION

The previous case was initially chosen to explore the process of back-pressuring, or changing the outflow boundary condition. The exit static pressure ratio was set to 11.62 which should keep the terminal shock supercritical, or well downstream of the inlet throat.

At this pressure ratio of 11.62, the solution did not reach any form of steady state solution. In examining the solution, the terminal shock's final position was found to oscillate around a fixed location, figure 15. This solution was obtained using the PROTEUS code with turbulent viscosity. From the freestream entrance plane to nearly one throat height downstream of the aft edge of the centerbody bleed slot, the Mach number contours remain constant with respect to computational time. Just downstream, the terminal shock location first advances forward and then collapses back downstream. These results are for 'local' time stepping an so are not time-accurate. However, the failure of the shock location to converge to a steady position suggests an inherent flow instability.

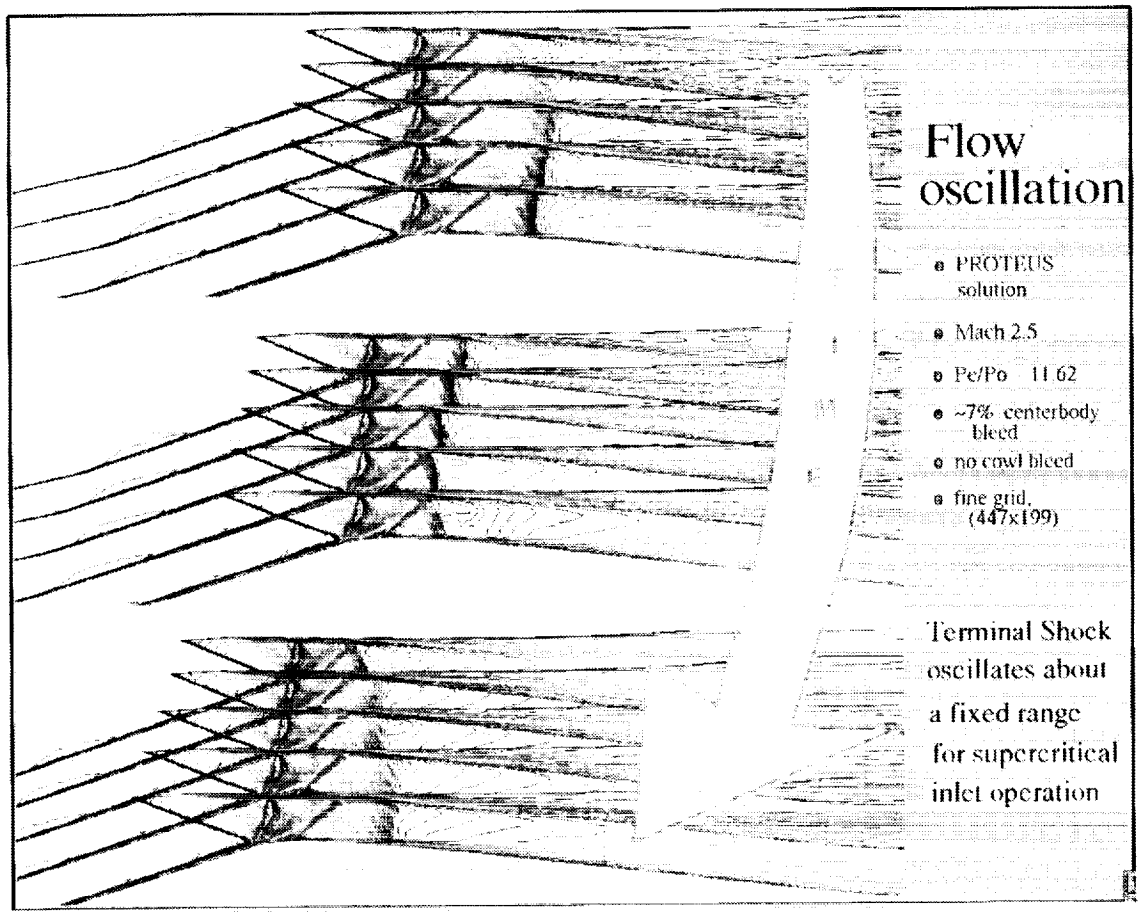

FIGURE 15. Backpressure and Flow Oscillation

FLOW OSCILLATION, STATIC PRESSURE DISTRIBUTION

Figure 16 shows the centerbody static pressure distribution for these cases. Again, the shock location indicated by the sharp pressure rise around X/R_c=3 first travels upstream, then downstream. Also, note the rise is much sharper for the upstream traveling shock compared to the downstream traveling shock. Integrated compressor face mass flow and mass-weighted total pressures are directly affected by the shock location and so also fluctuated for this cases. The flow unsteadiness is computationally intense; this sequence used 14 CRAY-YMP Cpu hours just to simulate a single period of the oscillation.

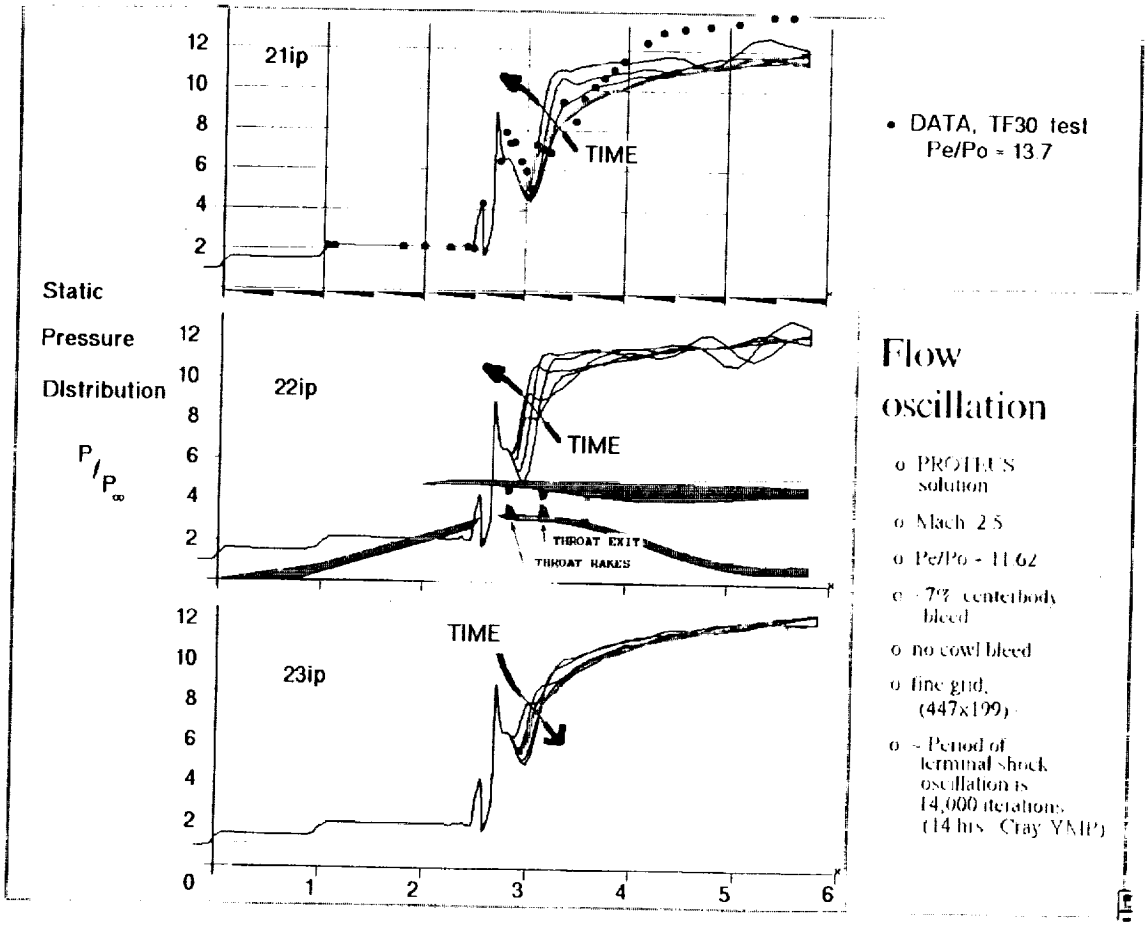

FIGURE 16. Flow Oscillation, Static Pressure Distribution

BACKPRESSURE TRANSIENTS, SUDDEN CHANGE

Figure 17 shows the computations for an exit pressure ratio of 13.6 that predicts unstarted inlet flow. This case was run with the PARC code with a sudden step change from 11.62 to 13.6 across a single computational time step. The Mach contours track the normal shock as it travel upstream, across the bleed slot and ultimately upstream of the cowl lip indicating inlet unstart.

The sudden change of pressure induces transient accelerations that can, (and in this case do), cause total pressures within the inlet to exceed the freestream total pressure. As mentioned before, this disturbance is roughly analogous to the hammershock overpressure phenomena encounter during hard engine stalls. If a steady state solution is ultimately sought, any increase in total pressure can be construed as an indication of unsteady flow. Since both PROTEUS and PARC are solving the unsteady Navier-Stokes equation, albeit inaccurately in time, an overpressure can occur and extreme care must be taken to prevent overwhelming pressure oscillations that can cause inlet unstarts.

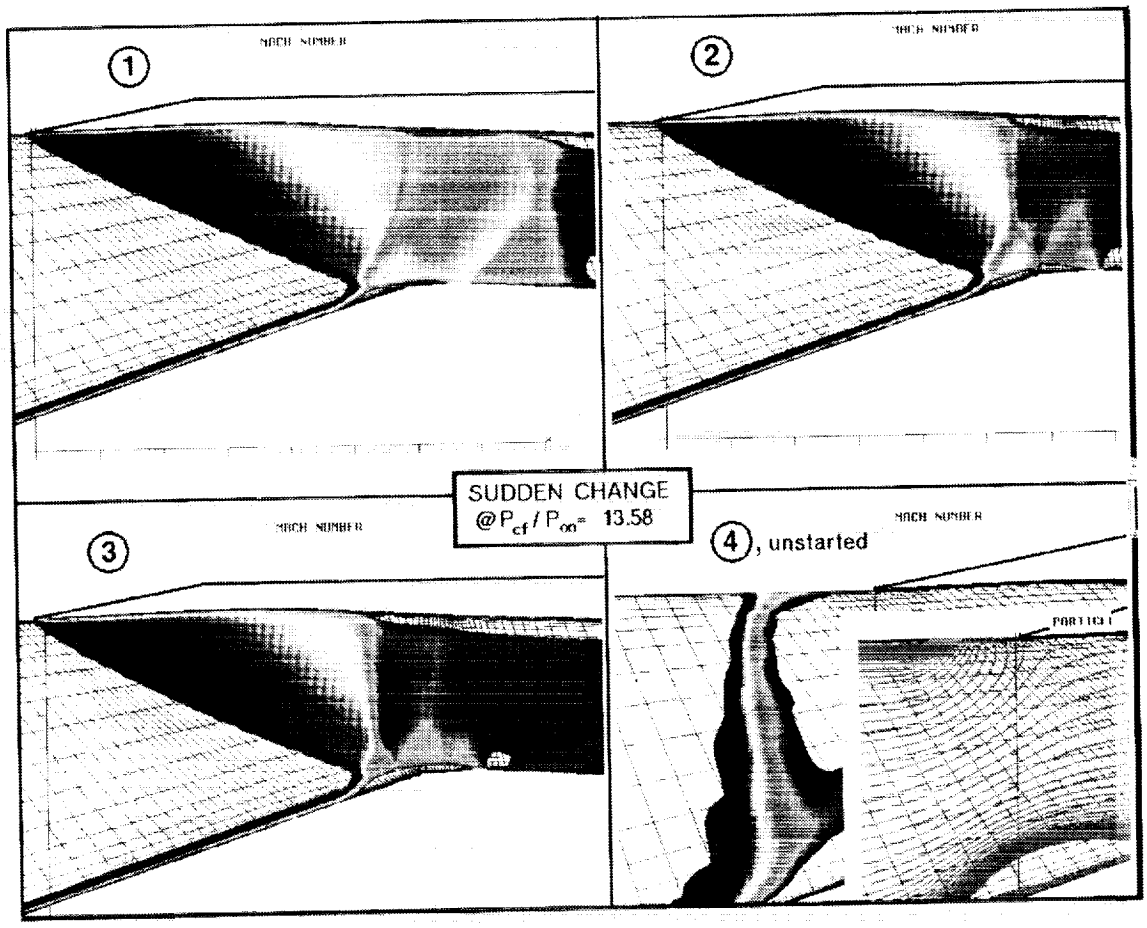

FIGURE 17. Backpressure Transients, Sudden Change

BACKPRESSURE TRANSIENTS, GRADUAL CHANGE

Because of the extreme sensitivity of shock position to the exit pressure boundary condition, further effort was made to gradually increase exit pressure and simulate critical inlet operation. PROTEUS was chosen for this effort due to two reasons. Since exit pressure can be changed gradually over a specified number of iterations, the problem of hammershock overpressure can be greatly reduced. The second reason for using PROTEUS lies with its more flexible bleed model. Both of these reasons were crucial to the successful simulation of critical inlet operation.

For this case the exit pressure was increased from 11.62 to 13.56 over 40,000 iterations, figure 18. Even with this slow change of pressure a slight overpressure occurs, travels upstream, and moves the terminal shock forward onto the bleed slot. The bleed boundary condition model, which was based on Hamed's velocity profile, reference 20, did allow the massflow to increase by ~50% during this terminal shock/bleed interaction. The shock eventually moved back downstream to the aft edge of the bleed slot but continued to oscillate thereafter. Also note that this case had a slightly modified inlet geometry. The cowl was translated downstream $X/R_c = .035$ in order to eliminate the separation bubble upstream of the centerbody shoulder. While not completely eliminated, the size of the separation has been dramatically reduced. The integrated massflow was 96.8% . Total pressure recovery was ~87.7% and the bleed massflow rate was ~3.4%. Also shown in the figure below is the comparison of static pressure distribution. The values have good agreement with measured overall inlet performance.

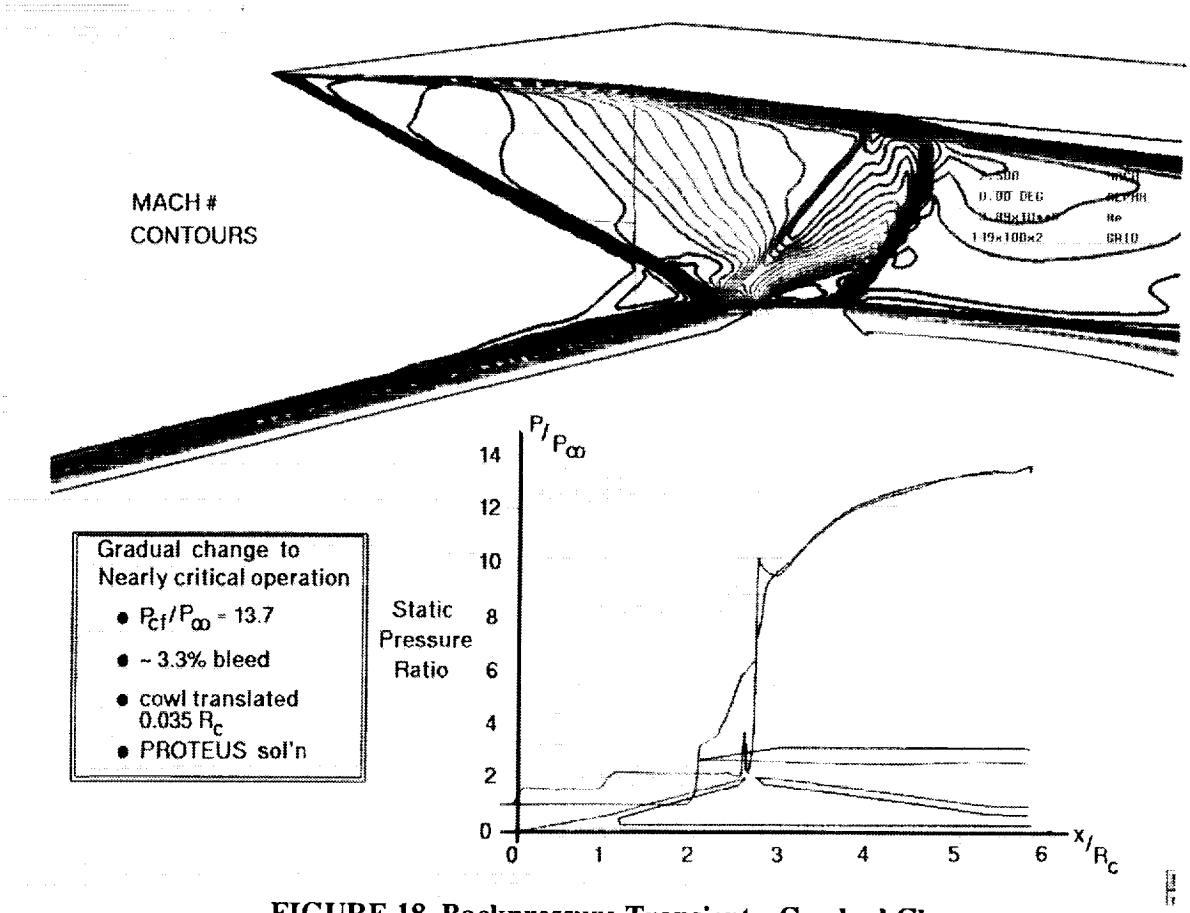

FIGURE 18. Backpressure Transients, Gradual Change

CONCLUDING REMARKS

The analysis of the VDC Inlet was undertaken, in part, to prepare for the experimental testing scheduled for the summer of 1992. This study has already impacted the testing by providing understanding of the bleed phenomena. It has also indicated areas of the inlet model in need of greater instrumentation. CFD investigation will continue throughout the preparation, testing, and reporting of the experimental program.

A series of analytical tools were applied to understand the flowfield in a supersonic inlet. These tools had varying degrees of success when compared to existing data from a wind tunnel test of the inlet geometry. Some of the major results are summarized below:

1) MOC analysis proved the inlet should operate well at off-design Mach numbers.

2) Elliptic Euler analysis failed due to instability in the centerbody flow separation, which led to an unstarted flowfield.

3) FNS viscous analysis predicted unstart for the design geometry without centerbody bleed, agreeing with experimental testing. Both analysis and testing agree that the design geometry will remain started at a bleed mass flow ratio, m_{bl}/m_o, of 2%.

4) For a supercritical inlet flowfield, FNS turbulent viscous analysis with bleed agreed well with experimental data forward of the centerbody bleed slot and regions of separated flow. Downstream of these regions the agreement is fair, pointing out deficiencies in the bleed and turbulence modeling.

5) FNS codes indicated an inherent unsteady flow oscillation of the terminal shock at a supercritical flow condition. This agrees with empirical experience that suggest that dynamic distortion increases as the terminal shock moves downstream from the inlet throat.

6) Both FNS codes failed to correctly predict the inlet recovery. Analytical predictions were ~1% below measured recoveries.

Further effort will be focussed in four areas:

1 - Further investigate critical and peak inlet operation by gradually increasing the compressor face pressure ratio up to the experimentally measured levels.

2 - Add the bleed passage to the calculation domain, thus eliminating bleed boundary condition modeling. With its multi-blocked grid formulation, the PARC code is ideally suited for this analysis.

3 - Implement the K-e turbulence model, (reference 21).

4 - Investigate the effect of cowl bleed on terminal shock/boundary layer interaction control.

REFERENCES

1. McLean, F. E.: "Future Directions of Supersonic Cruise Research", Supersonic Cruise Technology. NASA SP-472, 1985.

2. Wasserbauer, J. F.; Shaw, R. J.; and Neumann, H. E.: Design of a Very-Low-Bleed Mach 2.5 Mixed-Compression Inlet with 45 Percent Internal Contraction. NASA TM X-3135, 1975.

3.Neumann, H. E.; Wasserbauer, J. F.; and Shaw, R. J.: Performance of Vortex Generators in a Mach 2.5 Low-Bleed Full-Scale 45-Percent-Internal- Contraction Axisymmetric Inlet. NASA TM X-3195, 1975.

4. Wasserbauer, J. F.; Neumann, H. E.; and Shaw, R. J.: Distortion in a Full-Scale Bicone Inlet with 45 Percent Internal Contraction. NASA TM X-3133, 1975.

5.Wasserbauer, J. F.; Neumann, H. E.; and Shaw, R. J.: Performance and Surge Limits of a TF30-P-3 Turbofan Engine/Axisymmetric Mixed- Compression Inlet Propulsion System at Mach 2.5. NASA TP-2461, 1985.

6.Bowditch, D. N.: Some Design Considerations for Supersonic Cruise Mixed Compression Inlets. NASA TM X-71460, 1973.

7.Anderson, B. H.: Design of Supersonic Inlets by a Computer Program Incorporating the Method of Characteristics. NASA TN-D 4960, 1969.

8. Vadyak, J.; Hoffman, J. D.; and Bishop, A. R.: Calculation of the Flow Field in Supersonic Mixed-Compression Inlets at Angle of Attack using the Three-Dimensional Method of Characteristics with Discrete Shock Wave Fitting. NASA CR-135425, 1978.

9. Towne, C. E.; Schwab, J. R.; Benson, T. J.; and Suresh, A,: PROTEUS Two-Dimensional Navier-Stokes Computer Code-Version 1.0. NASA TM- 102552, 1990.

10. Cooper, G. K.; Sirbaugh, J. R.: PARC Code: Theory and Usage. AEDC-TR-89-15, 1989.

11. Sanders, B. W.: Dynamic Response of a Mach 2.5 Axisymmetric Inlet and Turbojet Engine with a Poppet- Valve-Controlled Inlet Stability Bypass System when Subjected to Internal and External Airflow Transients. NASA TP-1531, 1979

12. Hindash, I. O.; Bush, R. H,; and Cosner, R. R.: Computational Modeling of Inlet Hammershock Wave Generation. AIAA Paper 90-2005, 1990.

13. Pordal, H. S.; Khosla, P. K.; and Rubin, S. G.: Transient Behavior of Supersonic Flow through Inlets. AIAA 90-2130, 1990.

14. Weir, L. J.; Reddy, D. R.; and Rupp, G. D.: Mach 5 Inlet CFD and Experimental Results. AIAA Paper 89- 2355, July 1989.

15. Reddy, D. R.; Benson, T. J.; and Weir, L. J.: Comparison of 3-D Viscous Flow Computations of Mach 5 Inlet with Experimental Data. AIAA Paper 90-0600, 1990.

16. Rizzetta, D. P.: Numerical Simulation of a Supersonic Inlet. AIAA Paper 91-0128, 1991.

17. Hunter, L. G.; Tripp, J. M.; and Howlett, D. G.: A Mach 2.0 Plus Supersonic Inlet Study using the Navier-Stokes Equations. AIAA Paper 85- 1211, 1985.

18. Shigematsu, J.; Yamamoto, K.; and Shiraishi, K.: Numerical Investigation of Supersonic Inlet using Implicit TVD Scheme. AIAA Paper 90-2155, 1990.

19. Fujimoto, A.; Niwa, N.; and Sawada, K.: Numerical Investigation on Supersonic Inlet with Realistic Bleed and Bypass Systems. AIAA Paper 91- 0127, 1991.

20. Hamed, A., and Lehnig, T.: An Investigation of Oblique Shock/Boundary Layer Bleed Interaction. AIAA 90-1928, 1990.

21. Avva, R.; Smith, C.; and Singal, A.: Comparative Study of High and Low Reynolds Number Versions of k-e Models. AIAA Paper 90-0246, AIAA 28th Aerospace Sciences Meeting, Reno NV, January 1990.